Thin Solid Films – Elsevier Sequoia S.A., Lausanne – Printed in Switzerland

STRUCTURE AND ELECTRICAL PROPERTIES OF Au–SiO THIN FILM CERMETS

J. E. MORRIS*

Department of Electrical Engineering, University of Saskatchewan, Saskatoon, Saskatchewan (Canada)

(Received December 13, 1971; in revised form February 28, 1972)

SUMMARY

It is shown that deposition rate affects film properties of cermets indirectly through radiation heating of the substrate by the SiO source. The high temperature associated with fast depositions causes a reduction in the island dimensions, which are almost entirely dependent upon temperature and relatively independent of composition. It is also suggested that the SiO deposits as SiO_2 at higher temperatures. Both the film resistivities and activation energies of conduction compare very favourably with those predicted by the electrostatic charge activated tunnelling model of conduction.

INTRODUCTION

Although Cr–SiO has been found to be the most practical cermet (ceramic–metal) material for microelectronic resistors, its structure is too complex for a comparison of properties with simplified conduction theories[1–3]. In this paper we examine the related, but simpler, Au–SiO mixture for a basic study of cermet properties, since the close packed structure of stoichiometric SiO inhibits absorption effects[1] and the noble metal is not expected to form complex phases.

At low metallic concentrations the cermet structure consists of discrete metal islands in a continuous insulating medium[3, 4] and is similar to discontinuous metal film structures. The electrostatic charge activated tunnelling model of conduction[5–9], which has been applied to the discontinuous films, will be compared with the electrical properties of the Au–SiO films. In this model the electron tunnels from one island to the next with a modifying shift in the relative

* Now at: Physics Department, Victoria University of Wellington, P.O. Box 196, Wellington, New Zealand.

levels of the Fermi distributions caused by electrostatic charging of the islands. Film resistivity, ρ, may be expressed as

$$\rho = \rho_0 \exp \delta E/kT \tag{1}$$

where, by analogy with the discontinuous films,

$$\rho_0 \propto (h^3 B/8\pi m_e e^2) \sin(\pi BkT) \exp(A\bar{\phi}^{1/2}) \tag{2}$$

$$\delta E = (e^2/4\pi\varepsilon)(r^{-1} - (r+d)^{-1}) \tag{3}$$

$$= (e^2/4\pi\varepsilon R)\, 4p/(1-p^2) \tag{4}$$

provided $\delta E \gg kT \gg eV$, where

k is Boltzmann's constant
h is Planck's constant
T is the absolute temperature
m_e is the electronic rest mass
e is the electronic charge
ε is the dielectric constant of the medium ($= \varepsilon_r \varepsilon_0$)
r is the island radius
d is the interisland gap width
$R = 2r + d$
$p = d/R$
$\bar{\phi}$ is the average height of the potential barrier between islands
$A = (4\pi d/h)(2m^*)^{1/2}$
m^* is the effective mass of the tunnelling electron, introduced account for impurity trapping effects within the barrier[10–12]
$B = A/2\bar{\phi}^{1/2}$
V is the potential drop between islands.

This paper is concerned with the validity of the conduction model describ and the variation of film structure with deposition conditions.

EXPERIMENTAL METHODS

All films were co-deposited at pressures between 2×10^{-7} torr and 5×10 torr. The Corning 7059 substrates were heated from the rear by a NiCr w wound contact heater. Two series of experiments were made, A and B. W the first, or A series of films, deposition rate was uncontrolled as only cc positional effects were considered and only one film was deposited on e substrate. With the second, or series B films, deposition rates were preset appr mately to the desired values and eleven parallel films were deposited along e substrate. Electron microscopic examination was carried out for those film which could be lifted from the substrate after pre-etching in dilute H

lectron diffraction rings.

HERMAL EFFECTS OF DEPOSITION RATE

When the substrate is exposed to the depositing vapour stream, its temerature is known to rise [14–16]. The temperature of a metal plate in the substrate osition rises about 100 °C as SiO is deposited on it at normal rates. The temerature is reduced only slightly as the deposition rate is reduced to zero, suporting the conclusion of others that the temperature rise is due to radiation rom the vapour source and not to an energy transfer from the vapour. Depoition of Au at a maximum rate raises the temperature of a substrate face less han 5 °C and it is concluded that the primary influence on the substrate temerature rise will be the SiO source temperature, which is typically much greater han that of the Au source. It is expected then, that the influence of deposition ate on film properties may be interpreted in terms of increased substrate emperatures.

The increased substrate temperatures are indirectly observable for each eposition. For an initial substrate temperature T_0 and a film resistance deterined later as $R_0 \exp(\delta E_0/kT)$, the film resistance R_f measured at the end of eposition is always much less than $R_0 \cdot \exp(\delta E_0/kT_0)$. The final substrate temerature, T_f, may be found from $R_f = R_0 \exp(\delta E_0/kT_f)$. After deposition ceases ıe film resistance increases as the substrate temperature falls from T_f to T_0. deposition of Au is stopped and the SiO continues to deposit as a protective verlayer, the resistance remains absolutely constant since thermal equilibrium undisturbed, indicating that post-deposition annealing is not a significant ıctor.

ILM UNIFORMITY

Film conductance during deposition is directly proportional to deposition me, any deviation from linearity corresponding precisely to observed changes ı deposition rate or composition. Film structure is therefore uniform in cross ction, and the film temperature is constant after the small time (approx. 10 sec) t which the conductance–time plot intersects the time axis, which corresponds ith that predicted for thermal equilibrium to be established[16].

Non-uniformity is more pronounced in the film plane. When a metal subrate holder is used (as with series B films) it acts as a heat sink creating a thermal adient over the substrate surface. The effect is minimised by using a ceramic ıbstrate holder (as with series A films) but there is still a gradient effect proıced by heat-sinking effects in the heater contacts. In addition, the wire ound contact heater causes non-uniform heating along the substrate[17], which

can be eliminated by the use of a distributed radiation heater. The eleven films of each B deposition provide an estimate of the range of resistance variation typically less than one order of magnitude[17].

The distributed structure within the films is demonstrated by the nature of high voltage breakdown. A film resistivity $0.02 \exp(0.07e/kT)\ \Omega$ cm was converted to $1.32 \exp(1.40e/kT)\ \Omega$ cm at 200 V/cm as the low resistance paths burned out leaving a pattern of cracks in the film[17].

EXPERIMENTAL RESULTS

The experimental data for depositions A and B are given in Tables I and II. Arhennius plots of resistivity *versus* $1/T$ are presented in Fig. 1 and are of the form of eqn. (1). Good linearity and high derived values of δE are inconsistent with the simple tunnelling mechanism proposed by Henrickson *et al.* for the conduction process[18]. Non-linearity of the Arhennius plots has been observed

TABLE I

SUMMARY OF DEPOSITION PARAMETERS, COMPOSITION AND ELECTRICAL PROPERTIES OF SERIES A FILMS

No.	*Substr. Temp. (°C)*[1]		*SiO Rate (Å/sec)*	*ρ(Ω cm) at ambient*	*δE(eV)*	*ρ_0(Ω cm)*	*Island diameter 2r(Å)*
A1	204	27.0	4.90	1.3×10^5	0.347	8.9	19
A2	181	35.3	3.33	7.1×10^3	0.180	1.2	–
A3	166	57.4	0.89	3.5×10^5	0.277	5.9	–
A4	180	40.5	3.33	7.4×10^3	0.199	0.74	–
A5	192	57.7	2.67	9.5×10^2	0.167	0.45	38
A6	191	61.9	2.15	60	0.099	0.30	–
A7	183	63.2	3.11	37	0.082	0.27	38
A8	180	67.7	2.67	16	0.070	0.22	46
A9	180	63.7	3.33	15	0.069	0.24	38
A10	180	74.5	3.55	3.0	0.072	0.044	23
A11	180	76.7	2.67	7.3	0.053	0.074	–
A12	180	83.5	1.78	2.7	0.042	0.11	65
A13	180	89.4	2.15	1.4	0.061	0.050	57
AA[4]	Amb	46.4	4.17	9.3×10^3			
AB	Amb	58.8	6.22	1.1×10^4	~0.13	~890	28
AC[2,6]	Amb	~85	~0.9	0.12	~0.015	~3.0	80
AD[4]	Amb	69.5	4.22	13			
AE	Amb	60	3.33	1.6×10^3	~0.08	~22	46
AF[3-5]	Amb	~70	~5.2	3.75×10^{-4}			

Notes: 1. Estimated before deposition by measurement at symmetrical face of substrate–heater–substrate sandwich.
2. SiO Xtal malfunction—estimated rate from source current.
3. SiO Xtal malfunction—estimated rate from rate before malfunction.
4. Contacts lost in low temperature test.
5. Positive TCR.
6. Resistance changes upon admission of air. ρ_{amb} prior to admission, ρ_0, δE after admission.

BLE II

IMARY OF PROPERTIES OF SERIES B FILMS AS FUNCTIONS OF COMPOSITION AND DEPOSITION RATE

n	*SiO Rate (Å/sec)*	*% Au (wt)*	$\rho_{amb.}$ *(AVO) (Ω cm)*		*Centre (Keithley)*		*Comments*
			Centre	*Mean*	ρ_0 *(Ω cm)*	δE *(eV)*	
3	1.42	40.8	19	18	3.1	0.069	
9	3.02	51.9	0.90	0.80	0.19	0.066	
0	5.64	38.0	0.11	0.090	0.050	0.053	
1	0.98	32.4	2.7	2.6			Series AE and TCR Bad contact
7	1.55	39.6	1.4	1.7	0.95	0.015	
8	2.89	49.0	0.65	1.1	0.15	0.038	
9	5.56	46.5	0.40	0.70	0.064	0.072	
0	10.3	51.0	17	8.5	2.3	0.117	
3	1.15	71.4	0.47	2.0	0.17	0.040	
4	2.80	65.7	0.24	0.23	0.054	0.053	
5	5.16	67.6	0.060	0.055	0.015	0.055	
6	10.8	66.7	0.049	0.35			No bond to Al for temp. test
24	1.69	68.7	0.085	0.065			Series AE and TCR Anneals
						0.030	Distrib. Parallel
0	2.71	74.7	0.12	0.075	0.025	0.039	AE's
1	5.46	74.7	0.030	0.032	7.5×10^{-3}	0.037	Distrib. Parallel
						0.026	AE's
25	1.96	72.5	5.5×10^{-3}	2.7×10^{-3}			Series AE and TCR Anneals
26	2.31	82.0	0.020	0.023	0.011	0.018	
27	4.26	82.3	0.060	0.036	0.023	0.023	
21	1.42	85.1	3.75×10^{-5}	4.4×10^{-5}			$R = 7.3$ at 0 °C TCR = +0.015
22	2.67	85.4	5.00×10^{-3}	7.18×10^{-3}	5.75×10^{-3}	0	Anneals but maintains TCR = 0
23	4.58	87.0	7.0×10^{-4}	7.0×10^{-4}			Parallel AE and TCR Anneals

vith the B depositions but generally seems to involve series or parallel effects Table II). Differential expansion between the gold contacts and the cermet film which adheres well to the substrate due to the SiO content) causes contact problems in the low temperature testing necessary for films deposited at ambient emperature. B films were all deposited with the same power applied to the substrate heater.

Film resistances do not change upon admission of air to the vacuum system, with condensation of water directly on the film or over periods of months on the shelf[17]. Noise levels in the films are below detection level[19, 20]. There is a decided non-ohmic effect with conductance approximately proportional to the square root of applied field[21]. No differences in structure, ρ_0 or δE have been noted between deposition with or without applied fields[22].

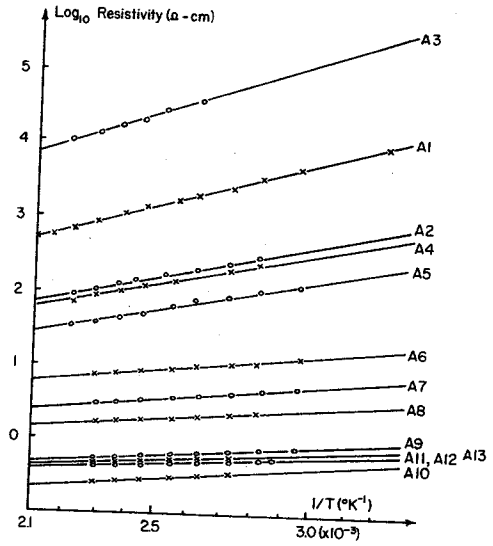

Fig. 1. Film resistivity as a function of temperature.

ANALYSIS OF EXPERIMENTAL RESULTS

Temperature Effects

Resistivity, ρ, is plotted for series A films in Fig. 2 as a function of co position and again in Figs. 3 and 4 where it has been separated into the co ponents ρ_0 and δE. It is apparent that much of the experimental scatter is rela to deposition rate. Figure 5 shows that $2r$ depends upon both deposition r and substrate temperature and is apparently independent of composition. F any assumed uniform film structure, p is determined by composition. ρ_0 therefore expected to decrease and δE to increase slightly with increasing depo tion rates and substrate temperatures (Fig. 3 and 4). These trends are more mark for series B films (Figs. 6 and 7) where deposition rates were controlled. (T anomalous ringed points will be ignored.)

Conduction Model

It has been shown by others[23] that the theoretical and experimental valu of δE are in agreement. Little attention has been paid, however, to the ρ_0 ter which must also be considered to confirm the conduction theory. Plotting theoret cal *versus* experimental values of δE, ε_r may be determined for evaluation of th model. Similarly, a plot of log ρ_0 *versus* d will yield $m^*\bar{\phi}$, which may be compare with expected values.

A problem exists with the determination of d from transmission electro micrographs which are projections of three dimensions on two. It is preferre

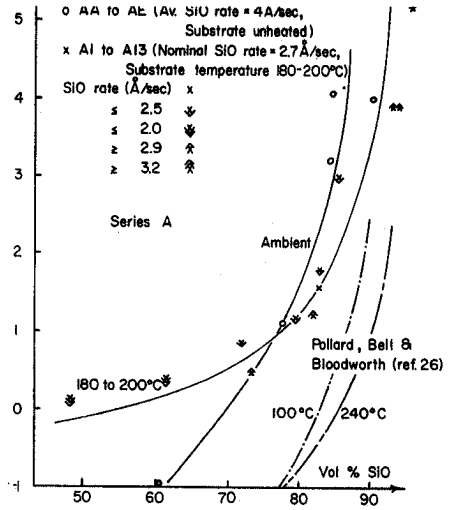

Fig. 2. Film resistivity at ambient temperature as a function of composition (Series A).

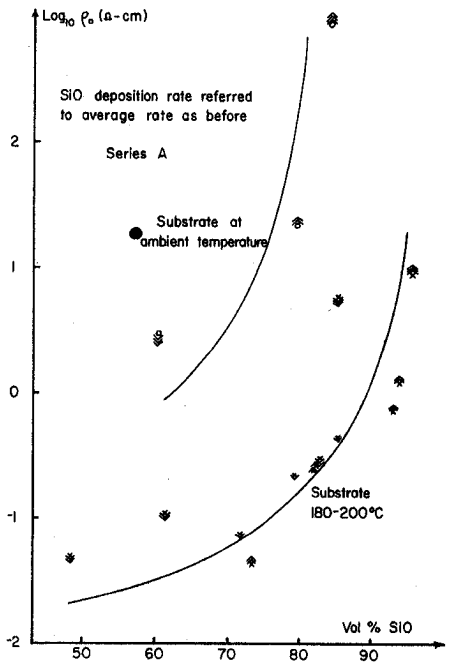

Fig. 3. Variation of ρ_b with film composition for heated and unheated substrates (Series A).

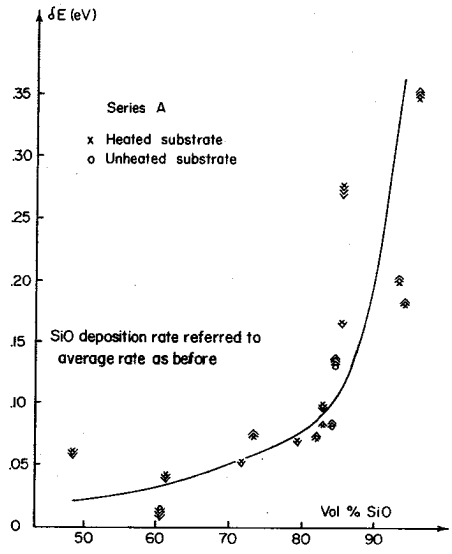

Fig. 4. Variation of δE with film composition for heated and unheated substrates (Series A).

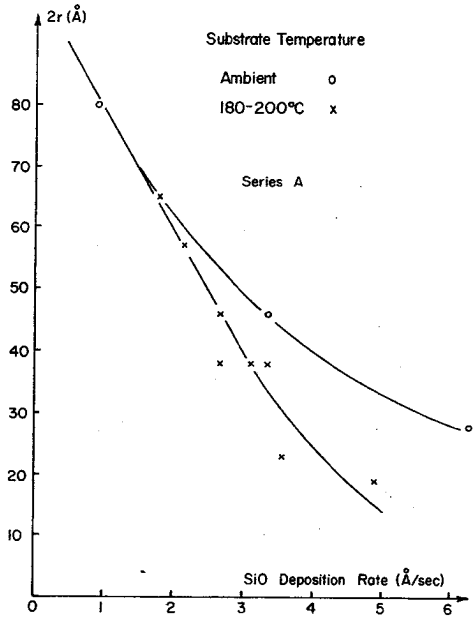

Fig. 5. Variation of $2r$ with SiO deposition rate (Series A).

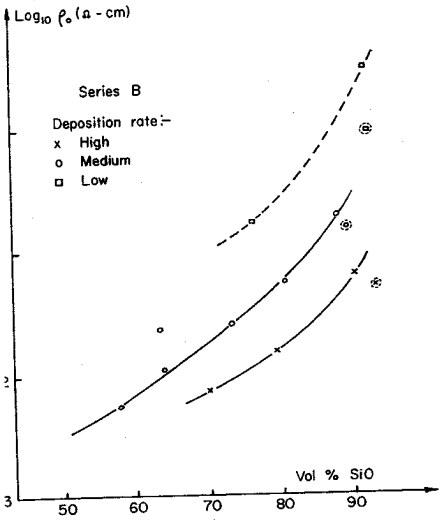

Fig. 6. Variation of ρ_0 with film composition for various deposition rates (Series B).

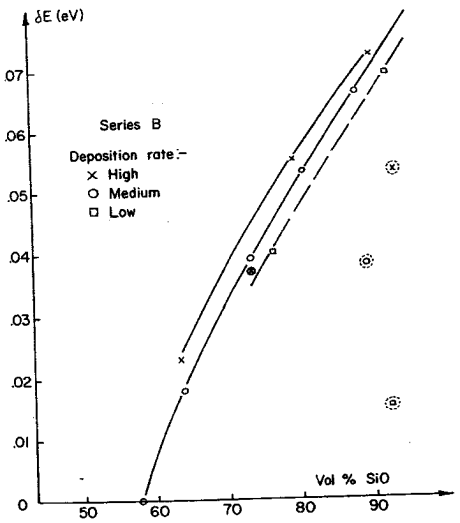

Fig. 7. Variation of δE with film composition for various deposition rates (Series B).

that d be determined using a theoretical value of p which is derived, with certain approximations, from the film composition. (A) First, the metal is assumed to be confined to identical spherical islands in a regular array. (B) This regular array is represented in turn by simple crystal lattice configurations for the sake of simplicity (*e.g.* simple cubic (s.c.), face centred cubic (f.c.c.), body centred cubic (b.c.c.) and diamond types). (C) Neugebauer[24] has proposed that SiO deposits

as SiO_2 with the excess Si forming gold silicides. The cermet composition ha therefore been considered as both Au–SiO and Au/Si–SiO_2 to cover both struc tures.

With these assumptions, the onset of metallic continuity within the film may also be predicted. With the s.c. structure, for example, $p = 0$ when th proportion of metal in the film by volume equals $\pi/6$. Table III lists the predicte

TABLE III

SUMMARY OF COMPARISON OF ELECTRICAL PROPERTIES WITH FILM STRUCTURE

Series	*Derived Param.*	*Assumed Dielec*	*Assumed Structure*			
			diamond	*s.c.*	*b.c.c.*	*f.c.c.*
–	Theoretical wt. % Au for $p = 0$	SiO	80%	90%	94%	95%
		SiO_2	8%	76%	90%	93%
A	ε_r	SiO	2.9	3.9	4.8	5.0
		SiO_2	—	0.8	1.8	1.5
B	$\varepsilon_r \cdot 2r$(Å)	SiO	340	250	210	225
		SiO_2	—	130	110	100
A	$m^*\bar{\phi}$ (xm_e·eV)	SiO	0.058	0.096	0.014	0.016
		SiO_2	—	1.1	0.091	0.175
B	$m^*\bar{\phi}(2r)$ (xm_e·eV·Å)	SiO	40	25	22	20
		SiO_2	—	510	440	380

Series A figures for films deposited at 180 °–200 °C.
Series B figures for medium deposition rate ($2r$ expected to be constant).

critical composition for each structure along with derived experimental value of ε_r and $m^*\bar{\phi}$. It is significant that the plots of log ρ_0 *versus* d for series A and o log ρ_0 *versus* $p(1-p)^{-1}$ $(=d/2r)$ for series B show good linearity. This resul supports the tunnelling part of the conduction theory. All values of ε_r are in th expected range but it appears that the optical value may be applicable[8] if th insulating phase is actually SiO_2[24]. The results for $m^*\bar{\phi}$ are not unreasonable For typical values of $\bar{\phi}$[23], however, m^* is generally lower than anticipated[1] implying significant trapsite densities.

Use of the four structural models is justified in part by the results whic support the validity of the conduction model in three independent features, (a) th onset of metallic properties, (b) ρ_0 and (c) δE, the last of which has been considere by others with the same conclusion. An additional observation supports the use c the four models as approximations of the real structure. The plot of δE *versu* $p(1+p)^{-1}$ for series B films of a single deposition rate ($2r$ constant) should b linear and pass through the origin. If the calculated value of n is higher or lowe

the origin (at low p) and intersect one axis or the other. Both such curvatures at low p and corresponding intersections were observed with the models employed which therefore include an effective approximation of film structure.

THERMAL ANNEALING

Annealing characteristics for two films are shown in Figs. 8 and 9. In both cases annealing decreases ρ_0 and increases δE which also becomes more distributed

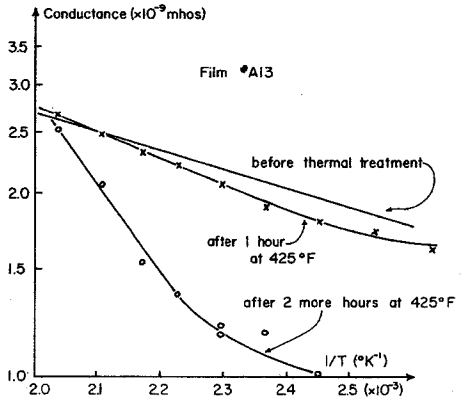

Fig. 8. Thermal annealing of a high resistivity film.

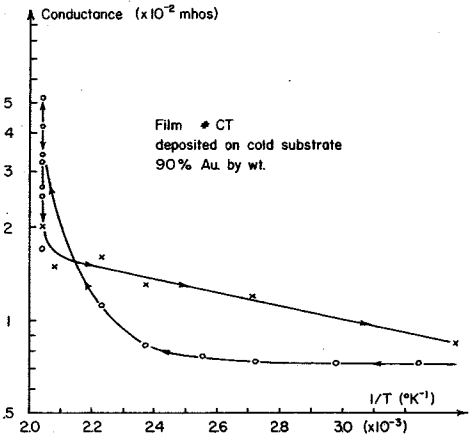

Fig. 9. Thermal annealing of a low resistivity film.

(Fig. 8). Mass transport and island coalescence are negligible at temperatures below 600 °C[23, 25] and it is therefore postulated that the annealing mechanism creates new islands within the insulating phase. For two original islands of radius r, and separation d, the introduction of a new island of radius r_2, equi-

distant d_2 from each of the original islands, will modify the original resistivity ρ_1 to ρ_2 where, to a first order approximation,

$$\rho_1 \approx c_0 \exp(c_1 d_1) \exp(c_2/r_1 T) \quad (5$$

$$\rho_2 \approx c_0 \exp(c_1 d_2) [\exp(c_2/r_2 T) + \exp(c_2/r_1 T)] \quad (6$$

and therefore

$$\rho_2/\rho_1 \approx \exp - c_2(d_1 - d_2) [1 + \exp(r_2^{-1} - r_1^{-1}) c_2/T] \quad (7$$

At high temperatures $\rho_2 < \rho_1$, at low temperatures $\rho_2 > \rho_1$, *i.e.* ρ_0 decreases, δE increases and becomes distributed.

There are two possible mechanisms for the generation of new islands. If a small proportion of the Au content is dispersed in the dielectric it is expected to precipitate out at high temperatures. The low mobility at the temperatures employed will prevent aggregation, however, and the alternative is considered more likely. In this proposal it is noted that (a) some authors maintain that stoichiometric SiO is best regarded as a suspension of Si in SiO_2[26] and (b) the SiO_2 being a stable configuration is likely to form at higher temperatures, allowing excess Si to precipitate from the SiO. The new islands are therefore probably Si or Au–Si. Individual free Si atoms will probably also act as trap sites leading to small values of m^*.

The decrease in $2r$ at high temperature was observed by Pollard *et al.*[27] but with additional compositional influences. An opposite effect was noted by Miller *et al.*[23] with sputtered Au–SiO_2 films. The decrease in $2r$ and corresponding increase in island density is not predicted for high temperatures by simple nucleation theory[28] unless site density also increases. If Si precipitates from the SiO at high temperature the nucleation site density (Si atoms) will increase for SiO cermets, but not for sputtered SiO_2[23].

CONCLUSIONS

It has been shown that ρ_0 and δE agree within reasonable bounds with the predictions of the charge activated tunnelling theory of conduction. The deposition rate affects film properties indirectly by radiation heating of the substrate and island dimensions are primarily determined by the substrate temperature, gap widths being subsequently fixed by composition. The composition of the insulating phase is still in doubt but seems to tend to SiO_2 at higher temperatures, with release of Si. Reproducibility requires direct control of radiation from the SiO source and uniform substrate heating.

The author is indebted to G. Skopick and V. Meyer for technical assistance and to Dean A. D. Booth for his constructive criticisms. This work was supported by N. R. C. Grants A1616 and A8150.

REFERENCES

1 R. GLANG, *J. Vac. Sci. Technol.*, *43* (1966) 37.
2 R. GLANG, R. A. HOLMWOOD AND S. R. HERD, *J. Vac. Sci. Technol.*, *4* (1967) 163.
3 T. J. COUTTS, *Thin Solid Films*, *4* (1969) 429.
4 T. E. CHRISTEN AND J. G. HEWITT, *IEEE Proc. 20th Electronic Components Conf.*, (1970) 63.
5 C. A. NEUGEBAUER AND M. B. WEBB, *J. Appl. Phys.*, *33* (1962) 74.
6 R. M. HILL, *Proc. Roy. Soc. (London)*, *A309* (1969) 377 and references cited.
7 R. KIERNAN AND D. W. STOPS, *Nature*, *224* (1969) 907.
8 J. E. MORRIS, *5th Intern. Vac. Congr.*, Boston (1971); *J. Vac. Sci. Technol.*, *9* (1972) 437.
9 R. KIERNAN AND D. W. STOPS, *5th Intern. Vac. Congr.*, Boston (1971).
10 F. W. SCHMIDLIN, *J. Appl. Phys.*, *37* (1966) 2823.
11 R. H. BADERTSCHER, *Ph. D. Thesis*, University of Michigan, 1968.
12 A. MODINOS, *Surface Sci.*, *20* (1970) 55.
13 J. E. MORRIS, *J. Intern. Microstructure Anal. Soc.*, in press.
14 E. YODA, *Jap. J. Appl. Phys.*, *8* (1969) 191.
15 G. BREITWEISER, B. N. VARADARAJAN AND J. WAFER, *J. Vac. Sci. Technol.*, *7* (1970) 274.
16 D. D. THORNBURG AND C. M. WAYMAN, *J. Appl. Phys.*, *42* (1971) 4063.
17 J. E. MORRIS, *Ph. D. Thesis*, University of Saskatchewan, 1971.
18 J. F. HENRICKSON, G. KRAUSS, R. N. TAUBER AND D. J. SHARP, *J. Appl. Phys.*, *40* (1969) 5006.
19 K. HEAD, *Thin Solid Films*, *4* (1969) 153.
20 K. E. G. PITT, *Thin Solid Films*, *1* (1967) 173.
21 S. S. MINN AND J. PINGUET, *C.R. Acad. Sci. Paris*, *271* (1970) 915.
22 J. E. MORRIS, *Metallography*, *5* (1972) 41.
23 N. C. MILLER, B. HARDIMAN AND G. A. SHIRN, *J. Appl. Phys.*, *41* (1970) 307.
24 C. A. NEUGEBAUER, *Thin Solid Films*, *6* (1970) 443.
25 A. D. MCMASTER AND N. FUSCHILLO, *J. Non-Cryst. Solids*, *2* (1970) 307.
26 J. BEYNON, *Vacuum*, *20* (1970) 293.
27 J. K. POLLARD, R. L. BELL AND G. G. BLOODWORTH, *J. Vac. Sci. Technol.*, *6* (1969) 702.
28 C. A. NEUGEBAUER in L. I. MAISSEL AND R. GLANG (eds.), *Handbook of Thin Film Technology*, McGraw–Hill, New York (1970) and references cited.